

Attenuated muscle regeneration is a key factor in dysferlin-deficient muscular dystrophy

Yen-Hui Chiu[†], Mark A. Hornsey[†], Lars Klinge^{†,‡}, Louise H. Jørgensen, Steven H. Laval, Richard Charlton, Rita Barresi, Volker Straub, Hanns Lochmüller and Kate Bushby*

Institute of Human Genetics, Newcastle University, International Centre for Life, Central Parkway, Newcastle-Upon-Tyne NE1 3BZ, UK

Received January 23, 2009; Revised and Accepted March 11, 2009

Skeletal muscle requires an efficient and active membrane repair system to overcome the rigours of frequent contraction. Dysferlin is a component of that system and absence of dysferlin causes muscular dystrophy (dysferlinopathy) characterized by adult onset muscle weakness, high serum creatine kinase levels and a prominent inflammatory infiltrate. We have observed that dysferlinopathy patient biopsies show an excess of immature fibres and therefore investigated the role of dysferlin in muscle regeneration. Using notexin-induced muscle damage, we have shown that regeneration is attenuated in a mouse model of dysferlinopathy, with delayed removal of necrotic fibres, an extended inflammatory phase and delayed functional recovery. Satellite cell activation and myoblast fusion appear normal, but there is a reduction in early neutrophil recruitment in regenerating and also needle wounded muscle in dysferlin-deficient mice. Primary mouse dysferlinopathy myoblast cultures show reduced cytokine release upon stimulation, indicating that the secretion of chemotactic molecules is impaired. We suggest an extension to the muscle membrane repair model, where in addition to fusing patch repair vesicles with the sarcolemma dysferlin is also involved in the release of chemotactic agents. Reduced neutrophil recruitment results in incomplete cycles of regeneration in dysferlinopathy which combines with the membrane repair deficit to ultimately trigger dystrophic pathology. This study reveals a novel pathomechanism affecting muscle regeneration and maintenance in dysferlinopathy and highlights enhancement of the neutrophil response as a potential therapeutic avenue in these disorders.

INTRODUCTION

Mutations in the dysferlin gene cause limb-girdle muscular dystrophy type 2B (LGMD2B), Miyoshi myopathy (1,2) and distal anterior compartment myopathy (3,4), collectively known as the dysferlinopathies. These conditions present typically with adult onset, progressive muscle weakness, highly elevated serum creatine kinase (CK) levels and a prominent inflammatory infiltrate in skeletal muscle (4–6). Dysferlin is named after its homology to the *Caenorhabditis elegans* fertility factor *fer-1* (2,7) involved in maturation of spermatids by fusing large vesicles with the plasma membrane. It is a class II membrane protein, containing multiple C2 domains (7,8), inferring that, like many C2 domain-containing proteins,

dysferlin is involved in vesicle fusion (2). Dysferlin interacts with various proteins including affixin, AHNAK, annexin A1 and A2, calpain-3 and caveolin-3 (9–11). The annexins and AHNAK are found in the enlargeosome, a calcium-regulated vesicle capable of rapid exocytosis (12–14) and both dysferlin and caveolin-3 traffic via the late endosomal compartment, from which the enlargeosome derives (15). A deficiency of membrane resealing in a mouse model of dysferlinopathy is consistent with the theory that dysferlin is involved in the fusion of vesicles from the enlargeosome with the plasma membrane (16,17). The ‘membrane repair hypothesis’ postulates that dysferlin is a key component of the muscle membrane repair system, which forms vesicle plugs over membrane lesions, maintaining cell homeostasis

*To whom correspondence should be addressed. Tel: +44 1912418737; Fax: +44 1912418666; Email: kate.bushby@ncl.ac.uk

[†]The authors wish it to be known that, in their opinion, the first three authors should be regarded as joint First Authors.

[‡]Present address: Department of Paediatrics and Paediatric Neurology, University Medical Centre Göttingen (UMG), Germany.

before the formation of new membrane (16,17). Recent studies have identified a further component of the muscle resealing apparatus, MG53, which responds early to membrane breaches and may serve to aggregate the membrane repair complex at the sarcolemma (18,19). Dysferlinopathy patients usually develop muscular dystrophy in adult life, following a period of good muscle performance. Mouse models of dysferlinopathy have a mild muscle phenotype, as do MG53 knockout animals. However, the link between the failure of membrane repair and the ultimate development of a muscular dystrophy remains unclear. We were therefore interested to explore how cumulative damage might be implicated in the development of disease and focused our attention on the next stage of muscle response to injury, whereby a muscle fibre undergoes regeneration. This process requires multiple cell types to work in synchrony, producing new contractile tissue in a few days, even after massive injury (20). Signalling from damaged tissue initiates rapid recruitment of neutrophils from the circulation (21). After 24–48 h, signalling from neutrophils and satellite cell populations attract monocytes (22), which are initially pro-inflammatory and phagocytose cellular debris. Activated satellite cells then start to proliferate and migrate to the injury site. Then, the monocyte population switches to an anti-inflammatory phenotype, differentiating into macrophages, which clear cellular debris and induce satellite cells to fuse (23). Studies have shown that the depletion of inflammatory cells has a marked effect on the eventual outcome of the regenerative process (23–26).

We demonstrate that dysferlin-deficient patients show an increase in immature fibres as defined by neonatal myosin (neo-MHC) labelling, suggesting that the regenerative process is delayed or incomplete in dysferlinopathy. Inducing muscle damage in the C57BL/10.SJL-*Dysf* mouse model of dysferlinopathy (27) demonstrates attenuated muscle regeneration. There is delayed early neutrophil recruitment, failure of clearance of necrotic fibres and a prolonged inflammatory infiltrate that correlates with a delay in the recovery of contraction force. The cumulative result of sequential impaired regeneration may be key to the ultimate development of a dystrophic phenotype in dysferlinopathy.

RESULTS

Dysferlinopathy patients show a higher number of immature fibres than muscular dystrophy controls

We assessed the number of immature fibres, as defined by neo-MHC expression, in 10 molecularly confirmed LGMD2B patients from the NCG rare neuromuscular disease service archives. Labelling on muscle sections was independently analysed blindly by two experienced investigators (R.B. and R.C.). The average percentage of fibres labelled with neo-MHC was compared with 16 LGMD2A patients, six dystrophinopathy patients and six LGMD2I patients (Fig. 1). Although the samples vary in patient age and stage of pathology, dysferlinopathy patients have a consistently higher percentage of neo-MHC-positive fibres (56.3%) than other muscular dystrophies, especially LGMD2A patients (13.9%; $P < 0.01$ Mann–Whitney). These fibres do not show utrophin

labelling, suggesting that these are not fibres at early stages of regeneration (Fig. 1).

Muscle pathology is mild but progressive in dysferlin-deficient C57BL/10.SJL-*Dysf* mice

We performed a thorough characterization of muscle pathology in the C57BL/10.SJL-*Dysf* mice (27) studying different muscle groups by histochemistry up to 1 year of age. Overt dystrophic changes are limited to specific muscle groups in older animals (data not shown). The tibialis anterior (TA) muscle was the target for our regeneration studies and studied for force generation. Even at 1 year of age, there is limited pathology in the TA, with some thickening of the perimysial connective tissue and a small number of central nuclei (Fig. 2A and B). Between 10 and 14 weeks of age, when the majority of our studies were performed, we observed only a small percentage of centrally localized nuclei. The limited overt pathology in the TA at this stage allowed us to investigate the effects of dysferlin deficiency in the absence of pre-existing dystrophic changes and secondary effects such as inflammation.

Mild muscle weakness is seen in C57BL/10.SJL-*Dysf* mice

We assessed C57BL/10.SJL-*Dysf*, C57BL/10 and *mdx* mice at 12–14 weeks of age using *in situ* force measurement. C57BL/10.SJL-*Dysf* animals had a reduced specific force (median 262 kN/m² in C57BL/10, 232 kN/m² in C57BL/10.SJL-*Dysf* and 178 kN/m² in *mdx*; $P < 0.05$ for each; Mann–Whitney, Fig. 2C). Maximum isometric twitch and tetanic forces in the C57BL/10.SJL-*Dysf* strain were not significantly reduced. The muscle was put through an eccentric (lengthening) contraction protocol (28), whereby a 40% lengthening contraction is used to damage the muscle. The dysferlin-deficient muscle showed no significant difference from control in the recovery of force generation after one (Fig. 2D) and two lengthening contractions (Fig. 2E), in contrast to *mdx*.

We also assessed dysferlin-deficient animals following eccentric exercise induced by exhaustive downhill running. The exhaustion times for C57BL/10.SJL-*Dysf* were reduced, although not significantly (C57BL/10 median 45 min, C57BL/10.SJL-*Dysf* 39 min, $P = 0.0532$ Mann–Whitney). Contrary to our previous report (27), serum CK levels were significantly elevated even without exercise (C57BL/10 median 480 IU/l, C57BL/10.SJL-*Dysf* 980 IU/l, $P < 0.002$ Mann–Whitney; Fig. 2F). In both strains, serum CK levels 1 day after exercise rose, returning to pre-exercise levels at day 4, before a second peak at 7 days post-exercise (Fig. 2F). Although this second peak is higher in C57BL/10.SJL-*Dysf* suggesting a persistence of muscle damage in this strain compared with control, the high variance in these observations makes further conclusions tentative.

Dysferlin-deficient mouse muscle is therefore slightly weaker than control, but is not more susceptible to immediate damage, showing none of the characteristic susceptibility to contraction-induced injury seen in *mdx*.

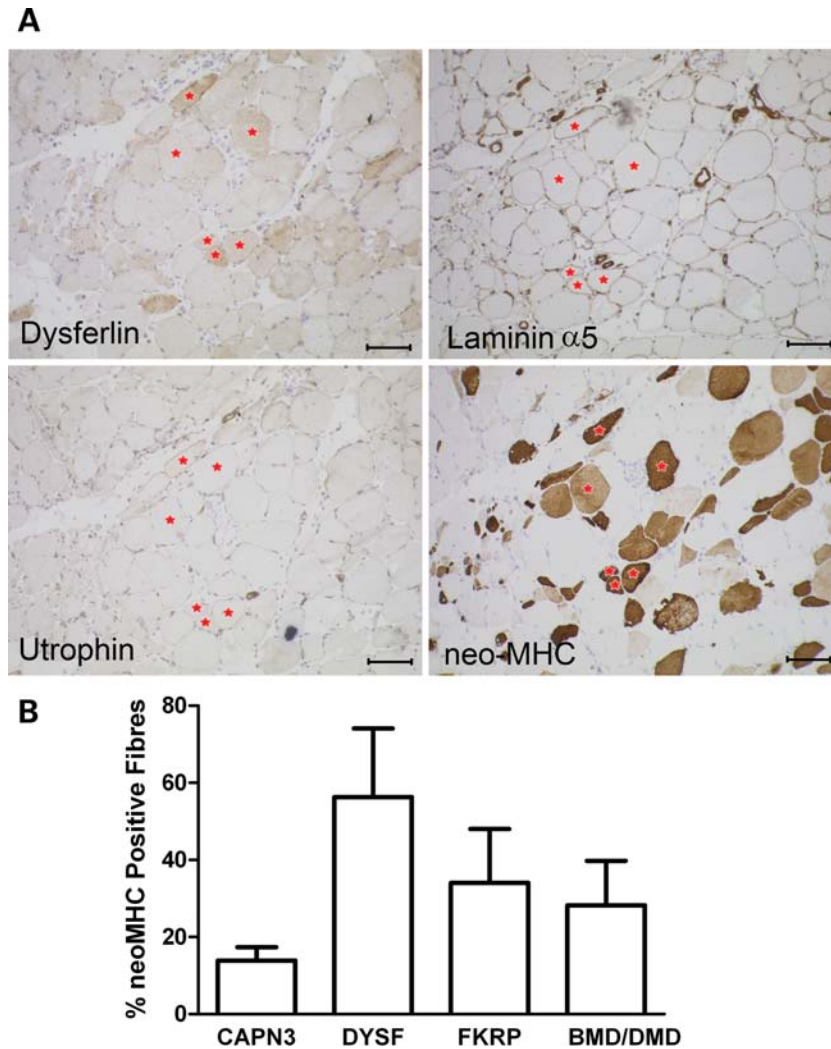


Figure 1. Dysferlinopathy patients show an excess of neo-MHC positive fibres. (A) Serial sections of a dysferlinopathy patient biopsy showing the characteristic extensive labelling for neo-MHC without up-regulation of utrophin or laminin- α 5 by immunohistochemistry. Red stars identify specific neo-MHC positive fibres in the serial sections. Scale bar is 100 μ m. (B) Mean percentage of fibres showing positive staining for neo-MHC in patient biopsies (\pm SEM). The causative gene of the patient groups is shown under the graph. Dysferlin $n = 10$, calpain-3 $n = 16$, FKRP and dystrophin $n = 6$.

Muscle regeneration is impaired and attenuated in C57BL/10.SJL-*Dysf* mice, with delay in recovery of muscle function after notexin treatment

C57BL/10 and C57BL/10.SJL-*Dysf* mice were injected with notexin (29,30) in the TA muscle of one hindlimb and the animals allowed to recover for up to 28 days. Sections of the muscle stained with H&E are shown in Figure 3A. Dysferlin-deficient muscle initially showed a lower concentration of mononuclear cells (3 days post-injection), but there was striking failure to resolve the inflammatory process, continuing beyond the point where the muscle was repaired in control mice. Later stage regenerating C57BL/10.SJL-*Dysf* muscle (7 and 14 days post-injection) is characterized by darkly staining red fibres, which remain anuclear and appear to provide foci for the ongoing inflammatory response. Alizarin red staining identifies abnormal sarcoplasmic accumulations of calcium. Such fibres persist in dysferlin-deficient muscle beyond the point

where they have been cleared in the control muscle (Fig. 3A). We conclude that notexin-induced regeneration is impaired in the dysferlin-deficient C57BL/10.SJL-*Dysf* mouse with delayed removal of necrotic fibres. To confirm that this is a feature of dysferlinopathy, the regeneration defect after notexin treatment has also been demonstrated in the *Dysf*^{tm1-Kcam} (16) dysferlin-deficient strain (Supplementary Material, Fig. S1A).

To look for correlation between the delayed removal of necrotic cells following injury and impairment of muscle function, *in situ* force measurement studies were performed on the notexin injected TA muscles of C57BL/10 and C57BL/10.SJL-*Dysf* mice after 7 and 14 days. Neither strain had recovered full muscle function even at 14 days post-injection. Recovery of the specific force was significantly impaired in dysferlin-deficient mice at 7 days post-notexin treatment (Fig. 3B). Specific force was reduced from 91% of wild-type levels in the untreated to 65% of

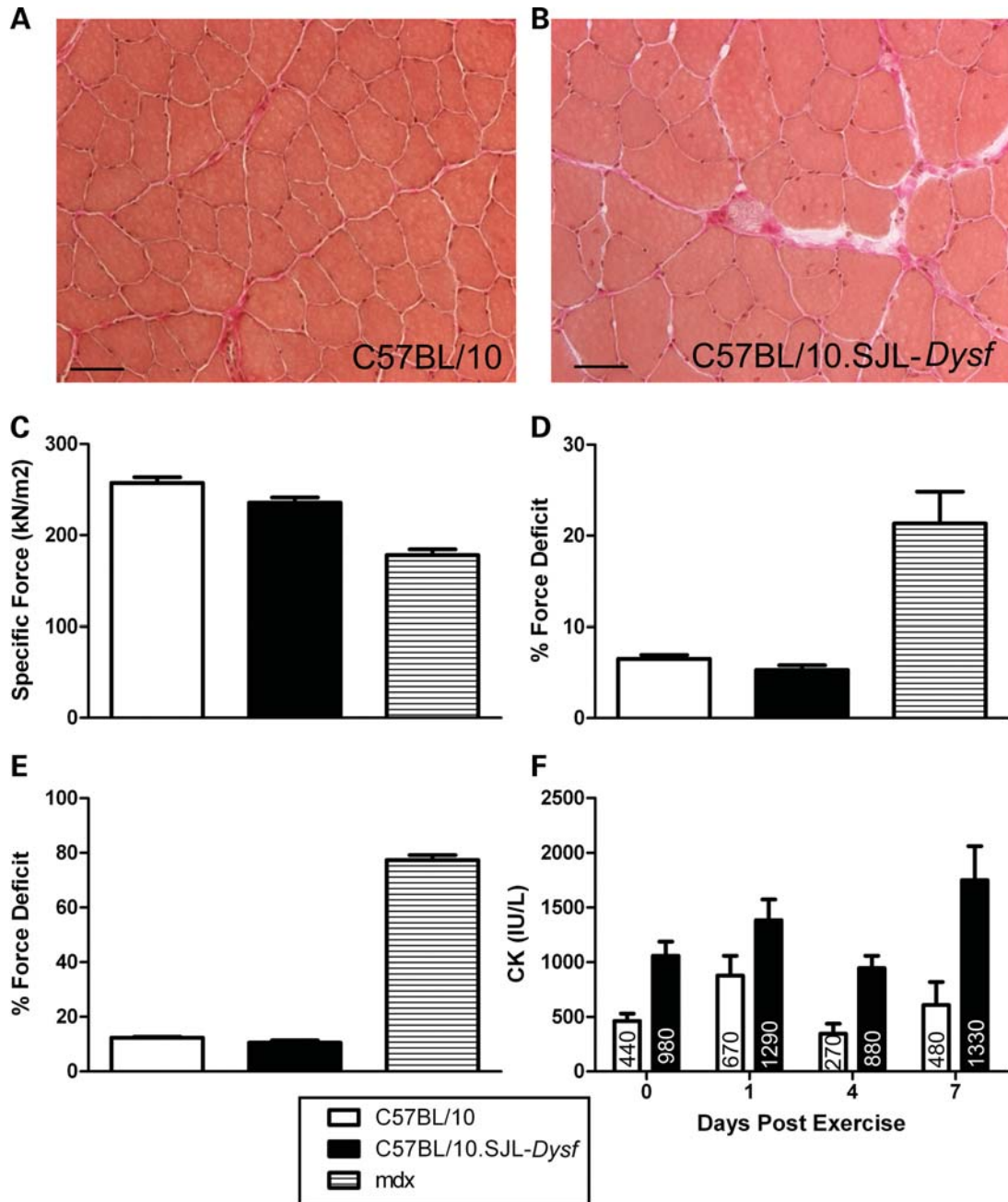


Figure 2. Characterization of the C57BL/10.SJL-Dysf mouse. Tibialis anterior muscle from 1-year-old C57BL/10 (A) and C57BL/10.SJL-Dysf (B) stained with van Gieson/Haematoxylin showing increased perimysial connective tissue in the dysferlin-deficient mouse, but limited pathology. Scale bar 50 μ m. (C) Specific force generation from C57BL/10 ($n = 7$), C57BL/10.SJL-Dysf ($n = 7$) and mdx ($n = 4$) mice. (D) Percentage drop in force following a single 40% lengthening contraction. (E) Percentage drop in force following two lengthening 40% contractions. (F) Serum creatine kinase 0, 1, 4 and 7 days post-exhaustive exercise. Median values are shown within the graph. Graphs show mean values (\pm SEM). C57BL/10 is represented by open bars, C57BL/10.SJL-Dysf by closed bars and mdx by hatched bars.

wild-type levels at 7 days after notexin injection. Median values of maximum isometric force were also significantly reduced at 14 days post-notexin and median values of both maximum isometric tetanic and specific force suggested that the recovery of these contraction parameters was also delayed; however, the results were not statistically significant (data not shown).

Repeated cycles of degeneration/regeneration result in a striking dystrophic phenotype in C57BL/10.SJL-Dysf mice

To further challenge the regenerative capacity of dysferlin-deficient muscles, C57BL/10.SJL-Dysf and C57BL/10 TA muscles of female mice aged 10–12 weeks were subjected to three rounds of notexin injection, 14 days apart. The muscles

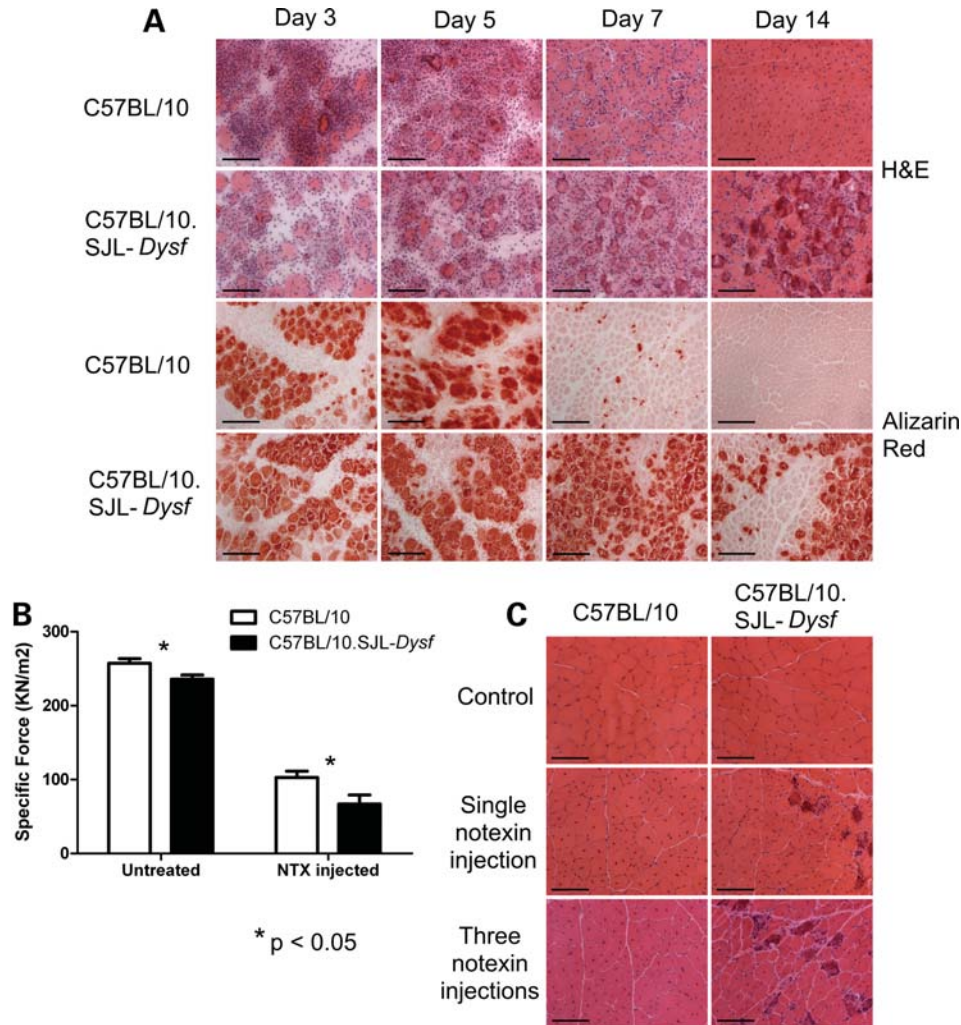


Figure 3. Muscle regeneration following notexin injury is impaired in dysferlin-deficient mice. (A) TA muscle from notexin injected mice after 3, 7 or 14 days of recovery and uninjected (control) were stained with haematoxylin and eosin or alizarin Red which detects intracellular calcium. (B) Mean specific force (\pm SEM) 7 days following notexin injection. Significant deficit in force recovery was found in the dysferlin-deficient strain ($P < 0.05$; $n = 5$ C57BL/10, $n = 6$ C57BL/10.SJL-Dysf). (C) H&E stained sections from C57BL/10 and C57BL/10.SJL-Dysf animals untreated (control), and following a single or three consecutive treatment(s) with notexin to induce muscle regeneration. Three injections of notexin in the C57BL/10.SJL-Dysf strain induce a marked dystrophic phenotype with variation in fibre size, inflammatory infiltration and necrotic fibres, whereas the control (C57BL/10) strain is capable of effective regeneration. Scale bars 100 μ m.

were harvested 3 or 8 weeks later. Three weeks following triple notexin treatment not only the C57BL/10.SJL-Dysf but also the control muscle was severely affected, showing equal extensive necrosis and inflammatory infiltrate (data not shown). However, the control muscle was able to fully repair by 8 weeks post-injection, whereas muscle from C57BL/10.SJL-Dysf showed a classical dystrophic pattern with fibrous tissue, variation in fibre size, an ongoing inflammatory process and darkly staining necrotic fibres (Fig. 3C). We conclude that repeated cycles of inflammatory insult and attenuated regeneration, act cumulatively to accelerate the development of a persistent dystrophic phenotype in the C57BL/10.SJL-Dysf muscle.

Satellite cell activation and myoblast fusion during regeneration appear normal in C57BL/10.SJL-Dysf mice

As activated satellite cells express dysferlin (31), we investigated the possibility that a failure to activate the satellite

cell population was responsible for impaired regeneration in dysferlin-deficient muscle. Quantitative PCR (qPCR) analysis of various markers of satellite cell activation and differentiation, *Myf5*, *Myog*, *Pax7* and *Cdk1b* (p27) showed no significant difference in any of these transcripts (Fig. 4A). The inherent variability of transcript levels at 3–4 days post-injection means that small differences at this stage would be difficult to detect without a much larger sample. However, the general pattern of expression of satellite cell markers is not markedly disturbed in the dysferlin-deficient strain suggesting that the defect in regeneration does not lie in an intrinsic defect of satellite cells. Indeed, injured muscles stained for desmin (a marker for myoblasts and early stage myotubes) show that C57BL/10.SJL-Dysf myoblasts fuse and form myotubes effectively (Fig. 4B). At 14 days, the difference in the regenerative process between the two strains appeared more to relate to failure of clearance of necrotic tissue than the ability to form new desmin positive fibres.

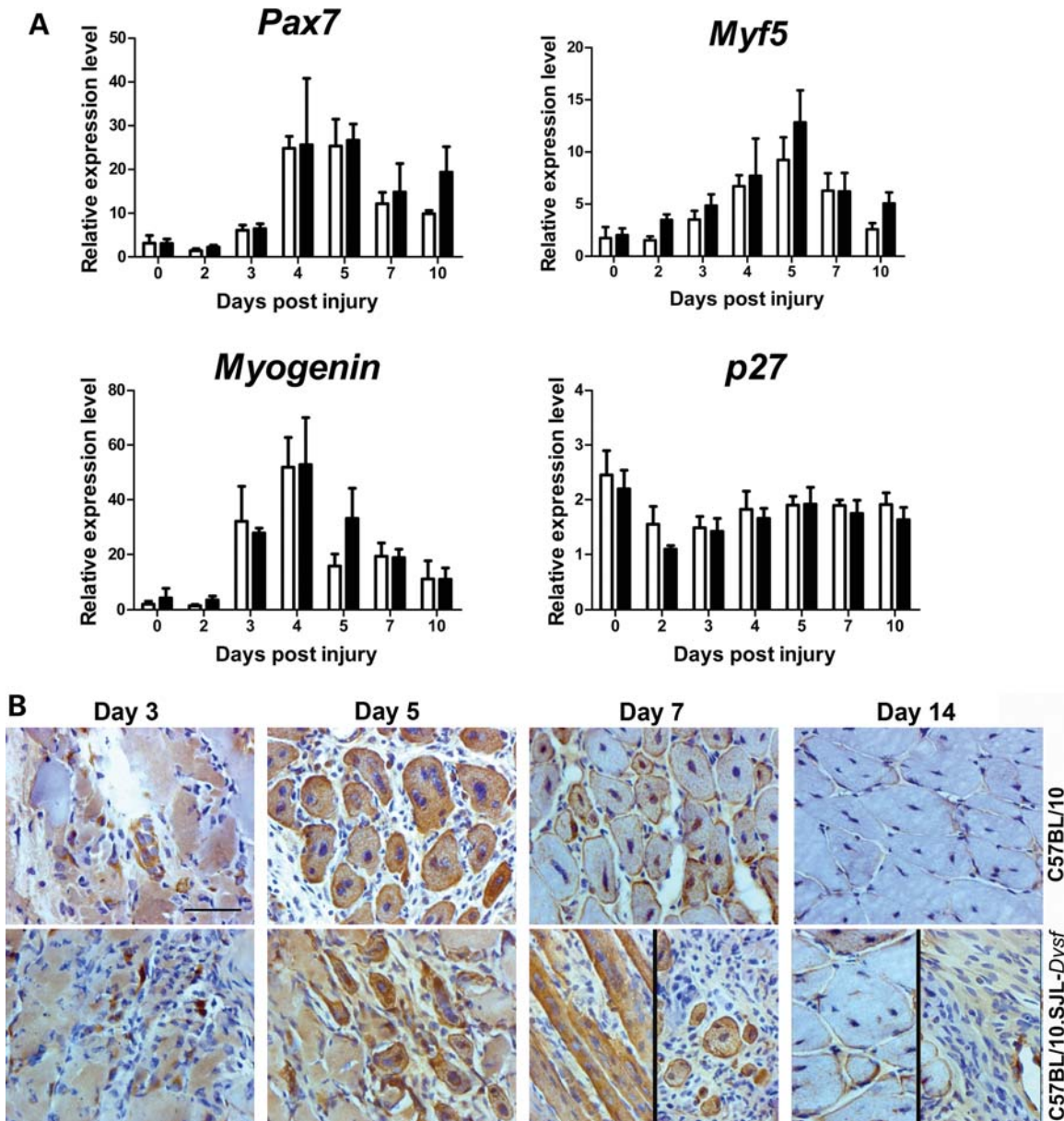


Figure 4. Satellite cell activation and fusion are not markedly perturbed during muscle regeneration in dysferlin deficient mice. (A) Quantitative RT-PCR analysis of transcripts involved in myogenesis and satellite cell fusion. There were no significant differences between the C57BL/10 (open bars) and C57BL/10.SJL-*Dysf* (closed bars) by two-way ANOVA. (B) Immunohistochemical analysis of desmin expression in muscle 3, 5, 7 and 14 days following notexin-induced regeneration identifies the fusing myotubes. Multiple small myotubes were present in the dysferlin deficient muscle, indicating the potential to fuse, although there was also necrotic fibres and extensive inflammatory infiltration. Variability in the appearance of the periphery (left panel) versus the centre (right panel) of the regenerating area is shown for C57BL/10.SJL-*Dysf* at day 7 and 14.

This prompted us to analyse the inflammatory cell component during regeneration in this model.

Dysferlin-deficient muscle shows early changes in the inflammatory cell infiltrate with reduced neutrophil recruitment following injury

Muscle sections at 3, 5 and 7 days after notexin injection were stained for Ly-6G, a neutrophil marker (Fig. 5A) and positive cells counted in seven random fields throughout the damaged area. The numbers of Ly-6G-positive cells at day 3 were

significantly reduced in dysferlin-deficient animals ($P < 0.01$). In order to confirm the attenuation of neutrophil recruitment, the inflammatory cell component of regenerating muscle was analysed by flow cytometry. Muscle from C57BL/10.SJL-*Dysf* and control animals through the course of notexin-induced regeneration was disaggregated, and the inflammatory cells were separated on CD45 expression. In both strains, the process of regeneration recapitulates a classical pattern with an early invasion of neutrophils, followed by a population of pro-inflammatory Ly-6C^{hi}, F4/80^{lo} monocytes recruited 1–3 days post-injection. These monocytes then

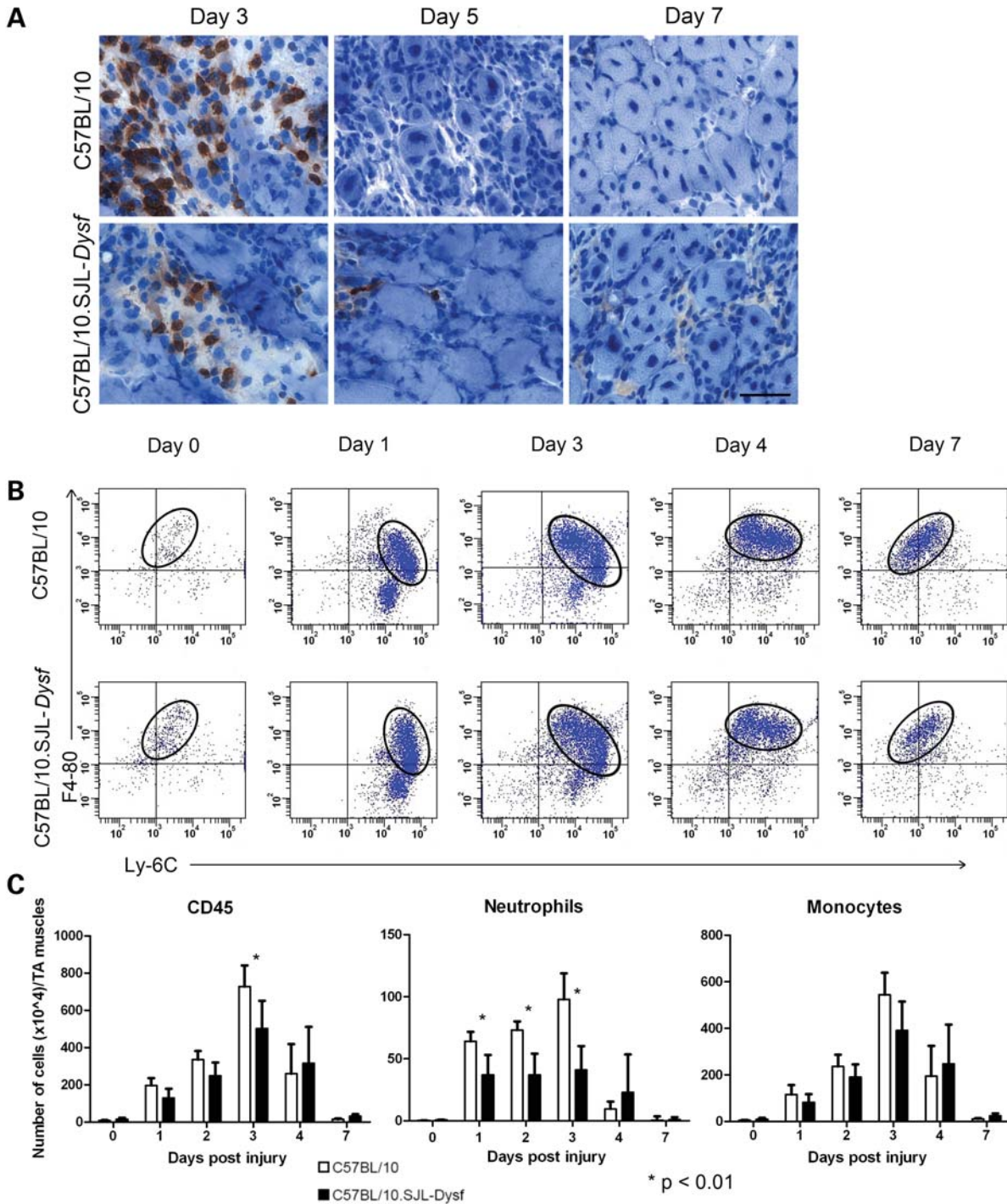


Figure 5. FACS analysis of notexin-induced regeneration indicates a reduced early neutrophil recruitment in dysferlin deficient muscle. (A) Muscle from C57BL/10 and C57BL/10.SJL-Dysf strains 3, 5 and 7 days after notexin-induced regeneration stained with an antibody against the neutrophil marker Ly-6G, developed with DAB (dark brown) and counterstained with haematoxylin to show nuclei (blue). Significantly ($P < 0.01$) fewer neutrophils were observed at day 3 in the C57BL/10.SJL-Dysf strain. Scale bar is 50 μm . (B) Frequency plots of CD45-positive mononuclear cells extracted from muscle 0, 1, 3, 4 or 7 days after notexin injection in either the C57BL/10 or the C57BL/10.SJL-Dysf strain. Each dot represents a single event from the cytometer. Circles identify the monocyte populations showing the shift from pro-inflammatory Ly-6C^{hi}/F4-80^{lo} into the macrophage precursor (Ly-6C^{lo}/F4-80^{hi}). (C) Numbers of CD45-positive cells, neutrophils and monocytes/macrophages extracted from the FACS data and normalized for mass of tissue. Significant ($P < 0.01$) differences between C57BL10 (open bars) and C57BL10.SJL-Dysf (closed bars) were found for total CD45 cells at 3 days after notexin injury and numbers of invading neutrophils at 1, 2 and 3 days after notexin injury.

switch *in situ* to become anti-inflammatory Ly-6C^{lo}, F4/80^{hi} macrophages, as the inflammatory phase is resolved 4–7 days post-injection (23). The switch from monocytes to macrophages appears unaffected in the dysferlin-deficient mice, and the qualitative pattern of inflammatory cell recruitment was similar in the two strains (Fig. 5B).

However, quantitative analysis of cell numbers showed a significant reduction in the number of neutrophils in the C57BL/10.SJL-*Dysf* mice at 1, 2 and 3 days post-injection compared with wild-type (Fig. 5C). There was also a significant reduction in the numbers of CD45-positive cells at 3 days post-injection. Monocyte populations also showed reduction in numbers at days 1–3, as would be expected since neutrophils secrete factors to recruit monocytes. In the early stages of regeneration (days 1–2), this difference was found specifically in the Ly-6C^{hi} monocyte population, although this failed to reach statistical significance. These represent the monocytes recruited from the circulation which then differentiate *in situ* (23) into the macrophage precursor (Ly-6C^{lo}) population. At day 3, the Ly-6C^{lo} monocyte population showed a significant reduction in dysferlin-deficient animals ($P < 0.02$). This indicates a generalized failure of monocyte recruitment with a concomitant reduction in the pro-macrophage (Ly-6C^{lo}) cell type at day 3 where phagocytosis of necrotic fibres peaks in the notexin model.

Needle wounding of C57BL/10.SJL-*Dysf* muscle confirms a defect in neutrophil recruitment

Needle wounding is a simpler and more confined event than notexin injection and we hypothesized that impaired neutrophil recruitment would also be apparent in needle wounded dysferlin-deficient muscles. Four TAs from C57BL/10.SJL-*Dysf* and control C57BL/10 mice were wounded with a hypodermic syringe needle and the muscle collected after 6 h. Serial sections of the muscle were immunostained for Ly-6G to identify the initial wave of infiltrating neutrophils. Histology showed reduced neutrophil recruitment to the site of injury in dysferlin-deficient muscle (Fig. 6A), and quantification of the number of infiltrating neutrophils around the site of injury confirmed this observation (Fig. 6B). The neutrophil recruitment defect after needle wounding has also been demonstrated in the *Dysf*^{tm1-Kcam} (16) dysferlin-deficient strain (Supplementary Material, Fig. S1B).

Reduced MCP-1 secretion by C57BL/10.SJL-*Dysf* myoblasts

Since cytokines are important for inflammatory cell recruitment, we hypothesized that dysferlin might play a role in the release of cytokines or chemokines. Primary myoblasts were derived from wild-type and dysferlin-deficient neonatal mice to investigate cytokine release in the two strains as a possible explanation for poor neutrophil recruitment. The cells were stimulated with 200 U/ml IFN- γ for 24 h before supernatant and cells were collected. MCP-1, MIP-2 and IL-6 secreted into the medium was measured by ELISA and normalized by total protein levels in the cell lysate. MIP-2 and IL-6 are not detectable at steady state in the medium or the cells of murine primary myoblasts. However, there was

a highly significant reduction in the MCP-1 released into the medium by stimulated dysferlin-deficient cells ($P < 0.001$) (Fig. 7). This indicates that there is an impairment of cytokine release in dysferlin-deficient muscle cells on direct stimulation. To confirm that the cytokine release in response to membrane wounding was also impaired this assay was repeated using 0.005% saponin to induce membrane wounds. MCP-1 secretion by dysferlin-deficient cells using this technique was also significantly ($P < 0.001$) impaired relative to the control (Fig. 7).

DISCUSSION

In 2003, Bansal *et al.* (16) demonstrated that dysferlin-deficient myotubes have a defect in membrane repair, leading to the hypothesis that failure to repair sarcolemmal damage following injury causes loss of cell homeostasis and cell death. Cumulative experience from the natural history of dysferlinopathy in patients and animal models and now also from the MG53 knockout demonstrates that the development of early severe muscular dystrophy is not a feature of defective muscle membrane repair. We became interested in a possible perturbation of the regenerative process both because it represents a longer term response to injury and also because of our observation of an increased number of immature fibres in dysferlinopathy patients compared with disease controls. We believe that the patch hypothesis of dysferlin function can be extended to put emphasis also on the content of the vesicles which fuse at the cell membrane after muscle injury, including neutrophil chemotactic factors (Fig. 8). Failure of the release of cytokines from damaged muscle could account for the impairment of inflammatory cell recruitment at an early stage of regeneration with subsequent incomplete muscle remodelling, resulting in the persistence of inflammatory cells and necrotic fibres, and over time, the development of muscular dystrophy.

This hypothesis is based on the known function of dysferlin and other ferlin proteins as well as the expression pattern of dysferlin in blood, which is restricted to the type II (non-classical) monocyte population (data not shown). Dysferlin is not expressed at an appreciable level in neutrophils, and so the deficient neutrophil response is unlikely to be due to functional differences between dysferlin-deficient and wild-type neutrophils. The dysferlin positive monocyte population is distinct from those which initially invade muscle following injury (23), so it is unlikely that monocyte expression of dysferlin is involved in the defective regeneration, since the type II monocytes are not involved until after the resolution of the inflammatory phase where regeneration of dysferlinopathic muscle is already abnormal. The well-established function of dysferlin in fusion of vesicles with the plasma membrane (10,16) and the observation of reduced cytokine release by dysferlin-deficient cells provide an alternative explanation, that part of the function of dysferlin is to release cytokines from internal vesicles in order to attract neutrophils to the site of injury. The model presented in Figure 8 is based on the assumption that the primary site of dysferlin action is the mature myofibre. An equally acceptable model could be conceived where dysferlin acts to secrete chemotactic factors

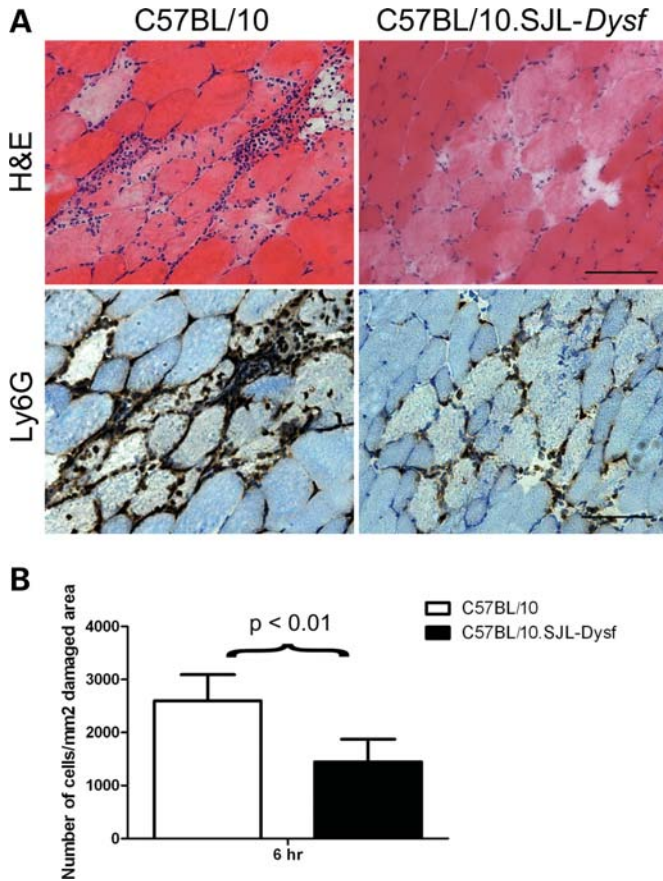


Figure 6. Ly-6G staining and needle wounding confirm a defect in neutrophil recruitment. (A) Needle wounded muscle from C57BL/10 and C57BL/10.SJL-Dysf was harvested 6 h after wounding and stained with H&E and by immunohistochemistry for the neutrophil marker Ly-6G. Scale bar is 50 μ m. (B) Counts of cells per unit area confirm the visual observation that significantly more neutrophils are present in C57BL/10 (open bars) than C57BL/10.SJL-Dysf (closed bars) 6 h after needle wounding.

from activated satellite cells or tissue resident macrophages (which derive from type II monocytes) and would also be found at the injury site, although not in the early stages when the neutrophil recruitment defect can already be demonstrated. This hypothesis remains tentative until some of the underlying assumptions have been tested.

Notexin injection is a well understood method for studying the process of muscle regeneration in animal models (23,30,32). Previous studies have indirectly suggested many ways that dysferlin could be involved in regeneration, including a possible role in satellite cell activation or fusion (31). Our data suggest the defect is not at the level of the satellite cell, as the expression pattern of genes involved in satellite cell activation and differentiation are not altered, and myoblasts appear to fuse normally. On the other hand, we show a significant reduction in neutrophil recruitment and a failure to clear necrotic fibres in regenerating dysferlin-deficient muscle: in keeping with the abnormal histology, there is reduced recovery of muscle force.

Following muscle injury, inflammatory cells are recruited to the injury site in an orderly manner. Neutrophils and monocytes coexist at the site of damage, suggesting that

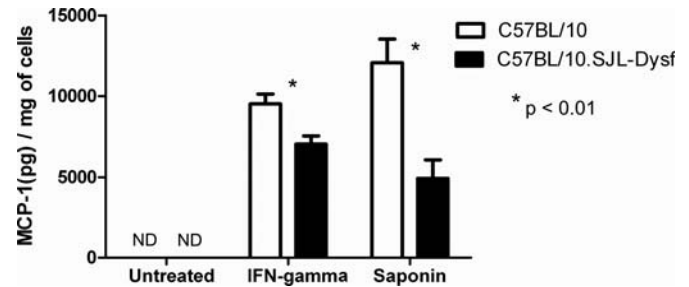


Figure 7. Dysferlin deficient primary myoblasts show impaired secretion of MCP-1 on stimulation. The concentration of MCP-1 was assayed by ELISA in the medium of primary myoblast cells derived from neonatal C57BL/10 (open bars) and C57BL/10.SJL-Dysf (closed bars) 24 h after stimulation with interferon gamma or treatment with 0.005% saponin. ND, not detected (MCP-1 was below the threshold for detection in the ELISA).

they have different, complementary functions. It is known that neutrophils produce oxidizing agents that can destroy cell membranes in the absence of other inflammatory cells (33), and blocking neutrophil function results in significantly diminished early tissue destruction (34). Monocytes are not responsible for membrane disruption, but their reparative functions are inhibited by the absence of neutrophils (35,36). Therefore, specific neutrophil functions are necessary for tissue repair and the interactions between neutrophils and monocytes appear essential to physiological regeneration. It is clear that the impaired neutrophil recruitment is not a consequence of the delayed regenerative process, since this effect precedes any perturbation in muscle regeneration and can also be observed shortly after needle wounding.

There is already direct evidence that the depletion of the neutrophil population impairs and attenuates muscle regeneration (24), leading to reduction in macrophage numbers and failure to clear necrotic fibres similar to our findings. The complete neutropenia induced in these studies is more extreme than the situation in dysferlinopathy, where only a partial reduction in neutrophil recruitment is observed. The moderate reduction in macrophage recruitment observed in our studies is also consistent with these data, where total neutropenia resulted in only an ~50% reduction in macrophage numbers. This is most likely due to the existence of neutrophil independent mechanisms of macrophage recruitment and a non-linear relationship between neutrophil signalling and macrophage response.

The inflammatory phase of muscle regeneration in our model persists beyond the stage where it has resolved in the control animals. This is entirely consistent with the human situation in dysferlinopathy where a persistent inflammatory infiltrate is common (6) possibly reflecting a failure of muscle remodelling following partial regeneration. We hypothesise that both in this model system and in the dystrophic patients, the persistent necrotic fibres provide foci for an ongoing inflammatory reaction. An increasingly pro-inflammatory milieu develops from successive rounds of poor regeneration, increasing the tissue load of both necrotic and inflammatory cells and directing myogenic cells towards a fibrotic fate (37,38).

We have confirmed previous data (32) that the established membrane repair defect in dysferlinopathic muscle does not appear to cause acute exercise intolerance which is in

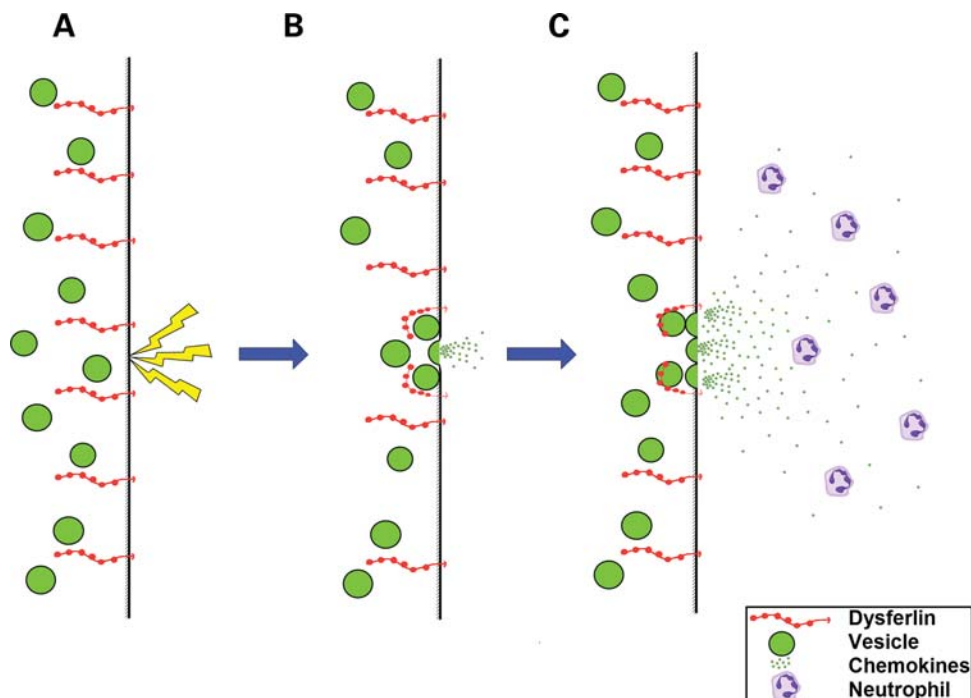


Figure 8. Hypothetical mechanism linking membrane repair with neutrophil recruitment in normal muscle. A membrane wound (A) such as physical injury or exercise induced tear, induces the calcium dependent fusion of vesicles with the sarcolemma (B) under the control of dysferlin. This releases vesicle contents, the hypothesized neutrophil chemotactic factors and reseals the membrane. Dysferlin continues to induce vesicle fusion (C) to set up a chemotactic gradient which directs neutrophils directly to the fibre, and specific region of the fibre, which was wounded.

contradistinction to the findings in the MG53 knockout mouse, despite an apparently comparable membrane resealing defect. Careful analysis of these animal models in the future may help to demonstrate the relative contributions of these different proteins to the process of repair and subsequent recovery. For example, it is possible to speculate that if the reduction in early neutrophil recruitment is specific to dysferlin deficiency, the normal neutrophil response in the MG53 knockout could contribute to the acute damage observed (18). Our finding of slight weakness, but no susceptibility to lengthening contractions in the dysferlin-deficient mice is consistent with this interpretation and the clinical situation, where patients generally develop weakness at a late stage and following a period of pre-symptomatic hyperCKaemia. This expanded model of disease pathogenesis explains a number of unusual features of the disease, including the late onset following a period of good muscle prowess with exercise tolerance and the extensive inflammatory process.

Previous studies have examined the role of dysferlin in monocytes (39,40) and found evidence of an increased phagocytotic activity (40). However, these authors examined the SJL/J strain and compared these animals with C57BL/6J. Genetic differences between these strains make it difficult to conclude that a global increase in phagocytotic activity is supported, especially given the strongly pro-inflammatory situation in SJL/J which would *a priori* be expected to increase the activity of phagocytes. Our studies using very similar techniques in C57BL/10-SJL.*Dysf* indicate no significant difference in the phagocytotic index when compared with the genetically equivalent C57BL/10 (data not shown).

These authors also examined phagocytes from dysferlinopathy patients. However, in these patients, there is commonly an ongoing inflammatory process in the muscle which would also be expected to increase phagocyte activity. The assay used, both in our laboratory and others, is a simple measure of the phagocyte ability to engulf fluorescent particles, whereas the process that we are examining in this study (the clearance of necrotic fibres by both neutrophils and macrophages) is much more complex, requiring tight control in order to initiate the orderly inflammatory process that degrades damaged tissue without damaging healthy cells. We believe that it is this cascade, rather than the process of phagocytosis itself which is defective here. It is, however, also important to consider that an additional factor in the resolution of regeneration might reside in the monocyte population, which also express dysferlin. Dysferlin is specifically expressed in the Ly-6C^{lo}, pre-macrophage population which is not recruited to the muscle until later in the regenerative process—a defect in this monocyte population therefore does not explain the early neutrophil recruitment defect but requires further investigation in the later stages of regeneration.

Although the precise mechanisms responsible for attracting inflammatory cells into damaged tissues remain unclear, mice with engineered mutations in MCP-1 or its receptor CCR2 display impaired skeletal muscle regeneration after injury (41,42). Interestingly, not only inflammatory cells but also satellite cells are responsible for cytokine release (43). We demonstrated that MCP-1 release from dysferlin-deficient myoblasts was significantly reduced relative to wild-type. It is already established that dysferlin translocates to the

membrane in response to injury and is responsible for the fusion of vesicles with the sarcolemma (10,16,44,45). Our findings implicate dysferlin in the process of cytokine/chemokine release upon muscle injury.

Establishing a link between any postulated molecular mechanism of disease and the end point of *in vivo* pathology is crucial to the development of targeted therapeutics. Our work emphasises failure of ongoing muscle regeneration and maintenance in addition to the acute response to sarcolemmal damage. Enhancement of the neutrophil response is a potential new therapeutic avenue for dysferlinopathy.

MATERIALS AND METHODS

Patients

Patients were identified for this study through the database of the Diagnostic and Advisory Service for Rare Neuromuscular Diseases based at the Muscle Immuno-Analysis Unit (MIU), Newcastle. All patients had a confirmed molecular diagnosis, had been analysed at the MIU and met ethical criteria for inclusion within the study.

Exercise-induced injury and CK analysis

We originally obtained dysferlin-deficient C57BL/10.SJL-*Dysf* mice from Professor Reginald Bittner (Medical University of Vienna). All strains of mice were housed under standard conditions and used according to the Animal Procedures Committee, Home Office, UK and local rules. To acclimatize the mice to the apparatus, mice were run gently downhill on a treadmill inclined at 15° for 10 min at 9 m/min on day 1, then 10 min at 10 m/min on day 2 and 10 min at 10 m/min on day 3. On day 4, the mice were run for 10 min at 10 m/min, at which point the speed was increased within a few seconds to 16 m/min. Mice were run to exhaustion at this speed and the time to exhaustion noted. Blood samples were taken via the tail vein and serum isolated for CK analysis.

In situ force measurement

This procedure was adapted from standard protocols (28,46). Mice were anaesthetized with an intra-peritoneal injection of hypnorm®/hypnovel®/water (1:1:2 by volume) at a dosage of 10 ml/kg. Under deep anaesthesia, the distal tendon of the TA muscle was dissected from surrounding tissue and the tendon tied with 4.0 braided surgical silk (Ethicon Inc.). The sciatic nerve was exposed and all its branches cut except for the common peroneal nerve (CPN), which innervates the TA muscle. The mouse was placed on a heated stage (Aurora Scientific Inc.) to maintain body temperature at 37°C. The TA tendon was attached to the lever arm of a 305C dual-mode servomotor transducer (Aurora Scientific Inc.).

TA muscle contractions were elicited by stimulating the distal part of CPN via bipolar platinum electrodes, using supra-maximal square-wave pulses of 0.02 ms (701B Stimulator; Aurora Scientific Inc.). Data acquisition and control of the servomotors were conducted using a LabView based DMC

program (Dynamic muscle control and Data Acquisition; Aurora Scientific Inc.).

After establishing the force–frequency relationship, we assessed the susceptibility of TA muscles to a lengthening contraction protocol. This consisted of stimulating the muscle at 180 Hz (the frequency that usually resulted in P_o) for 500 or 300 ms, then the muscle was lengthened by 40% of L_o at a velocity of $2L_t/s$. A second lengthening contraction identical to the first was administered 10 s later and maximum isometric force was measured 1 and 15 min later. At the end of the experiment, muscles were excised, weighed and prepared for histological analysis.

Muscle injury and muscle preparation

Notexin (50 μ l at 4 μ g/ml in 0.9% NaCl; Latoxan) was injected directly into the right TA of 8- to 12-week-old female mice using a 0.5 ml U-100 insulin syringe (the left TA was used as a non-injected control). For multiple injections, the animals were allowed to recover for 14 days between treatments and muscles were harvested 21 or 28 days following the final injection. The TA muscles were excised and rinsed in PBS and embedded in OCT. Serial 10 μ m sections were used for the histological analysis or immunohistochemical staining. Haematoxylin and eosin staining was used for morphological analysis and Alizarin Red S was used to detect the necrotic fibres. Images were taken using an AxioPlan II microscope (Carl Zeiss, Inc., USA) with Axiovision 4.6 software (Carl Zeiss MicroImaging, Inc.). Quantitative analysis of muscle regeneration was performed on the entire injured area. Ten fields (40 \times objective; Carl Zeiss MicroImaging, Inc.) were analyzed in each mouse, representing 300–400 fibres per muscle.

Immunohistochemistry

Longitudinal or transverse sections of 10 μ m were cut using a cryostat and kept at -80°C until further processing. Sections were fixed in 4% PFA/TBS for 15 min, followed by incubation in 3% H_2O_2 /TBS for 10 min to block endogenous peroxidase, and blocking of endogenous biotin (Avidin/Biotin Blocking System, DAKO). Sections were then incubated with 2% BSA/TBS for 30 min before application of primary antibody.

Sections were incubated with one of the following primary antibodies diluted in 2%BSA/TBS; biotinylated mouse anti-human desmin 1:25 (ARKTM Peroxidase kit (K3954, DAKO), clone D33, DAKO) at room temperature for 30 minutes or rat anti-mouse Ly6G 1:1000 (1A8, BD Pharmingen) overnight at 4°C. This was followed by anti-rabbit EnVision⁺-HRP-conjugated polymer (DAKO) or rabbit anti-rat biotinylated secondary antibody 1:200 for 30 minutes, then Streptavidin-HRP conjugate (DAKO) for 15 minutes and DAB⁺ substrate (Vector laboratories, Inc., Burlingame, CA) for development of peroxidase activity for 10 minutes. Counterstaining of nuclei was performed using Harris haematoxylin (Surgipath) followed by mounting of slides with Aquamount (VWR). Images were acquired using a Zeiss AxioPlan microscope coupled to an AxioCam camera and the AxioVision software.

qPCR

TA muscles were harvested before injury (day 0) and 2, 3, 4, 5, 7 and 10 days post-injection with notexin and total RNA was extracted using TRIzol, according to the manufacturer's instruction (Invitrogen). This was followed by reverse transcription of total RNA into cDNA using the Superscript III reverse transcriptase system, according to the manufacturer's instructions (Invitrogen). Relative expression levels of *Pax7*, *Myf5*, *Myog*, *Cdk1b* (p27) and reference genes *Hprt1* and *Pgk1* was determined using custom-made primer-probes (PrimerDesign Ltd., Southampton, UK) and the qPCR reactions were run on the ABI PRISM™ 7900 HT Real-Time PCR System (Applied Biosystems, Inc.). All reactions were run in triplicate on TA muscles ($n = 5$) for each time point for both C57BL/10 and C57BL/10.SJL-*Dysf* mice.

Raw data were extracted and analyzed in SDS2.1 (Applied Biosystems, Inc.) using automatic detection of Ct-values, followed by export to qBase (47). Here the Ct-values were quality checked, all triplicates were evaluated and a run was excluded if the difference in Ct within a triplicate >0.5 . For all analyses, the data was normalized to the expression of *Hprt1* and *Pgk1* (reference gene stability was determined using the geNorm Housekeeping gene selection kit plus additional custom-made reference genes (PrimerDesign Ltd.) and analyzed using the geNorm software (48), and the results were produced as relative expression level with lowest expression equal to one.

For the qPCR data, two-way ANOVA was used to determine if there was any statistically significant difference in relative expression levels over time for each analyzed mRNA between C57BL/10 and C57BL/10.SJL-*Dysf*. A P -value < 0.05 was considered significant.

Analysis of inflammatory cell recruitment

Inflammatory cell recruitment was analysed by flow cytometry. Mice (generally four per time point) were sacrificed 1, 2, 3, 4 and 7 days after notexin injection (non-injected mice were used as controls). Fascia of the TA was removed. Muscles were dissociated in PBS containing collagenase D 1.5 U/ml (Roche Diagnostics GmbH), dispase II 2.4 U/ml (Roche Diagnostics GmbH) and 2.5 mM CaCl₂, incubated at 37°C for 1 h, filtered and counted. Cells were stained with PerCP-Cy5.5-conjugated anti-CD45 (BD Biosciences), Alex647-conjugated anti-F4/80 (AbD Serotec) and FITC-conjugated Ly6C (BD Biosciences) antibodies. Analysis was performed with an LSRII cytometer (BD Biosciences). The numbers of monocytes and neutrophils were calculated as the total cells multiplied by the percentage of cells within the gate. Within this population, monocyte subsets were identified as either F4/80^{lo}/Ly6C^{hi} or F4/80^{hi}/Ly-6C^{lo}. Neutrophils were identified as F4/80⁻/Ly-6C^{int}. Total cell numbers were normalized to TA weight.

Primary myoblast culture and cytokine release assay

Primary myoblast cultures were isolated and cultured using standard techniques. Briefly, limb muscles were carefully removed from two to three neonatal mice and placed immediately

in PBS. In a laminar flow cabinet, the muscles were minced to slurry, treated with collagen/dispase/CaCl₂ solution, containing 1.5 U/ml collagenase D (Roche), 2.4 U/ml dispase II (Roche) and 2.5 mM CaCl₂, and incubated at 37°C for 25 min. After centrifugation for 5 min at 350g, the cells were resuspended in Ham's F-10 (Invitrogen) containing 20% fetal calf serum (Invitrogen), 2.5 ng/ml human basic fibroblast growth factor (Promega), 100 U/ml penicillin and 100 µg/ml streptomycin. The cells were cultured on collagen-coated flasks at 37°C in 5% CO₂ incubator and the growth medium was changed every 2 days. After four to five passages, most of the fibroblasts were eliminated from the culture and myoblasts were grown by replacing the F-10 based growth medium to F-10/DMEM-based primary myoblast growth medium (40% of Ham's F-10, 40% of DMEM, 20% fetal calf serum, 2.5 ng/ml basic fibroblast growth factor and 100 U/ml penicillin and 100 µg/ml streptomycin). For fusion assays, the medium was substituted with DMEM containing 5% horse serum and 100 U/ml penicillin and 100 µg/ml streptomycin. Primary myoblasts were cultured in a 24 well plate for 2 days before stimulation with 200 U/ml IFN-γ or wounding with 0.005% saponin. The medium and cells were harvested 24 h after stimulation and MCP-1 concentration was analyzed by ELISA (R&D Systems).

SUPPLEMENTARY MATERIAL

Supplementary Material is available at *HMG* online.

ACKNOWLEDGEMENTS

We would like to thank Neil Hamilton and Steve Smith for technical support, Dr Clare Jeffray and Dr Ian Gibb (Royal Victoria Infirmary, Newcastle) for performing the CK analysis, Professors John Harris and Clarke Slater for their advice concerning notexin, Dr Emilie Groen for an initial analysis of the LGMD2A data, Professor John Mathers for use of the treadmill, Ian Dimmick and Dr Rebecca Stewart for help with flow cytometry, Dr Andrew Roddam (University of Oxford) for help and advice with the statistical analysis and Dr Paul Sharp (Imperial College, London) for training in the *in situ* force measurement protocol. The authors also thank the National Commissioning Group (NCG) for supporting the diagnostic work in the LGMD population. This work was supported by Action Medical Research (UK), AFM (France), Deutsche Forschungsgemeinschaft (KL 1868/1-1 and 2-1 to L.K.), the Jain Foundation (USA), the Lundbeck Foundation (Denmark), Science City Newcastle, MRC (UK) as part of the MRC Centre for Neuromuscular Diseases and the Muscular Dystrophy Campaign (UK). Newcastle University is the coordinating partner of the TREAT-NMD network of excellence (EC 036825).

Conflict of Interest statement. None declared.

REFERENCES

- Liu, J., Aoki, M., Illa, I., Wu, C., Fardeau, M., Angelini, C., Serrano, C., Urtizberea, J.A., Hentati, F., Hamida, M.B. *et al.* (1998) Dysferlin, a novel skeletal muscle gene, is mutated in Miyoshi myopathy and limb girdle muscular dystrophy. *Nat. Genet.*, **20**, 31–36.

2. Bashir, R., Britton, S., Strachan, T., Keers, S., Vafiadaki, E., Lako, M., Richard, I., Marchand, S., Bourg, N., Argov, Z. *et al.* (1998) A gene related to *Caenorhabditis elegans* spermatogenesis factor fer-1 is mutated in limb-girdle muscular dystrophy type 2B. *Nat. Genet.*, **20**, 37–42.
3. Illa, I., Serrano-Munuera, C., Gallardo, E., Lasa, A., Rojas-Garcia, R., Palmer, J., Gallano, P., Baiget, M., Matsuda, C. and Brown, R.H. (2001) Distal anterior compartment myopathy: a dysferlin mutation causing a new muscular dystrophy phenotype. *Ann. Neurol.*, **49**, 130–134.
4. Nguyen, K., Bassez, G., Krahn, M., Bernard, R., Laforet, P., Labelle, V., Urtizberea, J.A., Figarella-Branger, D., Romero, N., Attarian, S. *et al.* (2007) Phenotypic study in 40 patients with dysferlin gene mutations: high frequency of atypical phenotypes. *Arch. Neurol.*, **64**, 1176–1182.
5. McNally, E.M., Ly, C.T., Rosenmann, H., Mitrani Rosenbaum, S., Jiang, W., Anderson, L.V., Soffer, D. and Argov, Z. (2000) Splicing mutation in dysferlin produces limb-girdle muscular dystrophy with inflammation. *Am. J. Med. Genet.*, **91**, 305–312.
6. Gallardo, E., Rojas-Garcia, R., de Luna, N., Pou, A., Brown, R.H. Jr and Illa, I. (2001) Inflammation in dysferlin myopathy: immunohistochemical characterization of 13 patients. *Neurology*, **57**, 2136–2138.
7. Achanzar, W.E. and Ward, S. (1997) A nematode gene required for sperm vesicle fusion. *J. Cell Sci.*, **110**, 1073–1081.
8. Davis, D.B., Doherty, K.R., Delmonte, A.J. and McNally, E.M. (2002) Calcium-sensitive phospholipid binding properties of normal and mutant ferlin C2 domains. *J. Biol. Chem.*, **277**, 22883–22888.
9. Huang, Y., de Morree, A., van Remoortere, A., Bushby, K., Frants, R.R., Dunnen, J.T. and van der Maarel, S.M. (2008) Calpain 3 is a modulator of the dysferlin protein complex in skeletal muscle. *Hum. Mol. Genet.*, **17**, 1855–1866.
10. Lennon, N.J., Kho, A., Bacskai, B.J., Perlmutter, S.L., Hyman, B.T. and Brown, R.H. Jr (2003) Dysferlin interacts with annexins A1 and A2 and mediates sarcolemmal wound-healing. *J. Biol. Chem.*, **278**, 50466–50473.
11. Matsuda, C., Kameyama, K., Tagawa, K., Ogawa, M., Suzuki, A., Yamaji, S., Okamoto, H., Nishino, I. and Hayashi, Y.K. (2005) Dysferlin interacts with affixin (beta-parvin) at the sarcolemma. *J. Neuropath. Exp. Neur.*, **64**, 334–340.
12. Borgonovo, B., Cocucci, E., Racchetti, G., Podini, P., Bachi, A. and Meldolesi, J. (2002) Regulated exocytosis: a novel, widely expressed system. *Nat. Cell Biol.*, **4**, 955–962.
13. Lorusso, A., Covino, C., Priori, G., Bachi, A., Meldolesi, J. and Chieregatti, E. (2006) Annexin2 coating the surface of enlargosomes is needed for their regulated exocytosis. *EMBO J.*, **25**, 5443–5456.
14. McNeil, A.K., Rescher, U., Gerke, V. and McNeil, P.L. (2006) Requirement for annexin A1 in plasma membrane repair. *J. Biol. Chem.*, **281**, 35202–35207.
15. Hernandez-Deviez, D.J., Howes, M.T., Laval, S.H., Bushby, K., Hancock, J.F. and Parton, R.G. (2008) Caveolin regulates endocytosis of the muscle repair protein, dysferlin. *J. Biol. Chem.*, **283**, 6476–6488.
16. Bansal, D., Miyake, K., Vogel, S.S., Groh, S., Chen, C.C., Williamson, R., McNeil, P.L. and Campbell, K.P. (2003) Defective membrane repair in dysferlin-deficient muscular dystrophy. *Nature*, **423**, 168–172.
17. Glover, L. and Brown, R.H. Jr (2007) Dysferlin in membrane trafficking and patch repair. *Traffic*, **8**, 785–794.
18. Cai, C., Masumiya, H., Weisleder, N., Matsuda, N., Nishi, M., Hwang, M., Ko, J.K., Lin, P., Thornton, A., Zhao, X. *et al.* (2009) MG53 nucleates assembly of cell membrane repair machinery. *Nat. Cell Biol.*, **11**, 56–64.
19. Cai, C., Masumiya, H., Weisleder, N., Pan, Z., Nishi, M., Komazaki, S., Takeshima, H. and Ma, J. (2008) MG53 regulates membrane budding and exocytosis in muscle cells. *J. Biol. Chem.*, **284**, 3314–33122.
20. Charge, S.B. and Rudnicki, M.A. (2004) Cellular and molecular regulation of muscle regeneration. *Physiol. Rev.*, **84**, 209–238.
21. Tidball, J.G. (1995) Inflammatory cell response to acute muscle injury. *Med. Sci. Sports Exerc.*, **27**, 1022–1032.
22. Chazaud, B., Sonnet, C., Lafuste, P., Bassez, G., Rimaniol, A.C., Poron, F., Authier, F.J., Dreyfus, P.A. and Gherardi, R.K. (2003) Satellite cells attract monocytes and use macrophages as a support to escape apoptosis and enhance muscle growth. *J. Cell Biol.*, **163**, 1133–1143.
23. Arnold, L., Henry, A., Poron, F., Baba-Amer, Y., van Rooijen, N., Plonquet, A., Gherardi, R.K. and Chazaud, B. (2007) Inflammatory monocytes recruited after skeletal muscle injury switch into antiinflammatory macrophages to support myogenesis. *J. Exp. Med.*, **204**, 1057–1069.
24. Teixeira, C.F., Zamuner, S.R., Zuliani, J.P., Fernandes, C.M., Cruz-Hofling, M.A., Fernandes, I., Chaves, F. and Gutierrez, J.M. (2003) Neutrophils do not contribute to local tissue damage, but play a key role in skeletal muscle regeneration, in mice injected with *Bothrops asper* snake venom. *Muscle Nerve*, **28**, 449–459.
25. Summan, M., Warren, G.L., Mercer, R.R., Chapman, R., Hulderman, T., Van Rooijen, N. and Simeonova, P.P. (2006) Macrophages and skeletal muscle regeneration: a clodronate-containing liposome depletion study. *Am. J. Physiol.*, **290**, R1488–R1495.
26. Tidball, J.G. and Wehling-Henricks, M. (2007) Macrophages promote muscle membrane repair and muscle fibre growth and regeneration during modified muscle loading in mice *in vivo*. *J. Physiol.*, **578**, 327–336.
27. von der Hagen, M., Laval, S.H., Cree, L.M., Haldane, F., Pocock, M., Wappler, I., Peters, H., Reitsamer, H.A., Hoger, H., Wiedner, M. *et al.* (2005) The differential gene expression profiles of proximal and distal muscle groups are altered in pre-pathological dysferlin-deficient mice. *Neuromuscul. Disord.*, **15**, 863–877.
28. Dellorusso, C., Crawford, R.W., Chamberlain, J.S. and Brooks, S.V. (2001) Tibialis anterior muscles in *mdx* mice are highly susceptible to contraction-induced injury. *J. Muscle Res. Cell Motil.*, **22**, 467–475.
29. Harris, J.B., Johnson, M.A. and Karlsson, E. (1974) Proceedings: histological and histochemical aspects of the effect of notexin on rat skeletal muscle. *Br. J. Pharmacol.*, **52**, 152P.
30. Plant, D.R., Colarossi, F.E. and Lynch, G.S. (2006) Notexin causes greater myotoxic damage and slower functional repair in mouse skeletal muscles than bupivacaine. *Muscle Nerve*, **34**, 577–585.
31. de Luna, N., Gallardo, E., Soriano, M., Dominguez-Perles, R., de la Torre, C., Rojas-Garcia, R., Garcia-Verdugo, J.M. and Illa, I. (2006) Absence of dysferlin alters myogenin expression and delays human muscle differentiation 'in vitro'. *J. Biol. Chem.*, **281**, 17092–17098.
32. Schertzer, J.D., Gehrig, S.M., Ryall, J.G. and Lynch, G.S. (2007) Modulation of insulin-like growth factor (IGF)-I and IGF-binding protein interactions enhances skeletal muscle regeneration and ameliorates the dystrophic pathology in *mdx* mice. *Am. J. Pathol.*, **171**, 1180–1188.
33. Nguyen, H.X. and Tidball, J.G. (2003) Interactions between neutrophils and macrophages promote macrophage killing of rat muscle cells *in vitro*. *J. Physiol.*, **547**, 125–132.
34. Brickson, S., Ji, L.L., Schell, K., Olabisi, R., St Pierre Schneider, B. and Best, T.M. (2003) M1/70 attenuates blood-borne neutrophil oxidants, activation, and myofiber damage following stretch injury. *J. Appl. Physiol.*, **95**, 969–976.
35. Grounds, M.D. (1987) Phagocytosis of necrotic muscle in muscle isografts is influenced by the strain, age, and sex of host mice. *J. Pathol.*, **153**, 71–82.
36. Toumi, H., Poumarat, G., Best, T.M., Martin, A., Fairclough, J. and Benjamin, M. (2006) Fatigue and muscle-tendon stiffness after stretch-shortening cycle and isometric exercise. *Appl. Physiol. Nutr. Metab.*, **31**, 565–572.
37. Brack, A.S., Conboy, M.J., Roy, S., Lee, M., Kuo, C.J., Keller, C. and Rando, T.A. (2007) Increased Wnt signaling during aging alters muscle stem cell fate and increases fibrosis. *Science*, **317**, 807–810.
38. Li, Y. and Huard, J. (2002) Differentiation of muscle-derived cells into myofibroblasts in injured skeletal muscle. *Am. J. Pathol.*, **161**, 895–907.
39. De Luna, N., Freixas, A., Gallano, P., Caselles, L., Rojas-Garcia, R., Paradas, C., Nogales, G., Dominguez-Perles, R., Gonzalez-Quereda, L., Vilchez, J.J. *et al.* (2007) Dysferlin expression in monocytes: a source of mRNA for mutation analysis. *Neuromuscul. Disord.*, **17**, 69–76.
40. Nagaraju, K., Rawat, R., Veszelovszky, E., Thapliyal, R., Kesari, A., Sparks, S., Raben, N., Plotz, P. and Hoffman, E.P. (2008) Dysferlin deficiency enhances monocyte phagocytosis: a model for the inflammatory onset of limb-girdle muscular dystrophy 2B. *Am. J. Pathol.*, **172**, 774–785.
41. Shireman, P.K., Contreras-Shannon, V., Ochoa, O., Karia, B.P., Michalek, J.E. and McManus, L.M. (2007) MCP-1 deficiency causes altered inflammation with impaired skeletal muscle regeneration. *J. Leukoc. Biol.*, **81**, 775–785.
42. Contreras-Shannon, V., Ochoa, O., Reyes-Reyna, S.M., Sun, D., Michalek, J.E., Kuziel, W.A., McManus, L.M. and Shireman, P.K. (2007) Fat accumulation with altered inflammation and regeneration in skeletal muscle of CCR2^{-/-} mice following ischemic injury. *Am. J. Physiol. Cell Physiol.*, **292**, C953–C967.
43. De Rossi, M., Bernasconi, P., Baggi, F., de Waal Malefyt, R. and Mantegazza, R. (2000) Cytokines and chemokines are both expressed by human myoblasts: possible relevance for the immune pathogenesis of muscle inflammation. *Int. Immunol.*, **12**, 1329–1335.

44. Klinge, L., Laval, S., Keers, S., Haldane, F., Straub, V., Barresi, R. and Bushby, K. (2007) From T-tubule to sarcolemma: damage-induced dysferlin translocation in early myogenesis. *FASEB J.*, **21**, 1768–1776.
45. Bansal, D. and Campbell, K.P. (2004) Dysferlin and the plasma membrane repair in muscular dystrophy. *Trends Cell Biol.*, **14**, 206–213.
46. Sharp, P.S., Akbar, M.T., Bouri, S., Senda, A., Joshi, K., Chen, H.J., Latchman, D.S., Wells, D.J. and de Belleruche, J. (2008) Protective effects of heat shock protein 27 in a model of ALS occur in the early stages of disease progression. *Neurobiol. Dis.*, **30**, 42–55.
47. Hellemans, J., Mortier, G., De Paepe, A., Speleman, F. and Vandesompele, J. (2007) qBase relative quantification framework and software for management and automated analysis of real-time quantitative PCR data. *Genome Biol.*, **8**, R19.
48. Vandesompele, J., De Preter, K., Pattyn, F., Poppe, B., Van Roy, N., De Paepe, A. and Speleman, F. (2002) Accurate normalization of real-time quantitative RT–PCR data by geometric averaging of multiple internal control genes. *Genome Biol.*, **3**, RESEARCH0034.